Heat Pipes for Cooling High Flux/ High Power Semiconductor Chips

M. T. North

C. T. Avedisian

Sibley School of Mechanical and Aerospace Engineering, Cornell University, Ithaca, NY 14853-7501

Results of an experimental study are reported which demonstrate the ability of heat pipes to simultaneously dissipate high heat fluxes and high total power at low surface temperatures. The application is to cooling high power density (and high total power) semiconductor chip modules. The two designs studied incorporate air or liquid cooling in the condenser sections. The air-cooled design consisted of a manifold base plate with a series of holes drilled in it each of which was lined with sintered copper powder which served as the wick. An array of wick lined tubes was attached normal to the plate and served as the condenser section. The other heat pipe was disk shaped and also had a sintered wick structure. Cooling water channels were placed over the entire periphery of the housing except in the region of heat input. Reported steady heat fluxes are up to 31 W/cm^2 corresponding to total power dissipation of up to 1400 W for the water cooled heat pipe and up to 47 W/cm^2 (900 W total power) for the air cooled heat pipe with surface temperatures under 100°C.

1 Introduction

The long-term performance reliability of microprocessor chips is mainly determined by the ability to maintain temperatures at the chip level to within acceptable limits during operation. These limits are generally under 100°C. The trend toward smaller chips and larger total powers has motivated research into more aggressive heat dissipation schemes than have been used in the past. Chip heat fluxes of 40 W/cm^2 are not uncommon in some mainframe computers, and even in the mini/microcomputer market fluxes of this level are being projected. Techniques based on single phase natural convection air flow are generally capable of dissipating heat fluxes of only several watts per square centimeter under 100°C, though analyses imply the potential for much higher fluxes using single phase forced convective cooling (Hanneman 1989). It has been suggested that liquid cooling, in particular techniques which incorporate phase change, is capable of meeting the projected needs of the electronics industry (e.g., Bergles 1988; Kraus and Bar-Cohen 1983).

A device which can combine forced air and phase change cooling is the heat pipe (Antonetti et al. 1989; Andros and Sammakia 1989; Waller 1985; Kraus and Bar-Cohen 1983). It dissipates heat by a cyclic process that involves evaporation and condensation of a self-contained coolant. Virtues of heat pipes for chip cooling applications are that the coolant and chip are not in direct contact with each other, and because heat dissipation is by evaporation of a liquid the potential exists for high operating fluxes at the heat source. A particularly useful viewpoint of a heat pipe is as a very high thermal conductivity path between the source (e.g., single or multichip module) and sink (e.g., cold plate or fin array). For example, using data from a cylindrically shaped heat pipe (Faghri and Buchko 1991; Ponnapan et al. 1989), the effective thermal conductivity between the evaporator and condenser section separated by a distance $L(k_{\text{eff}} \equiv QL/(A\Delta T)$ where Q and A are the heat input to the evaporator section and the heat pipe cross-sectional area, respectively) can be shown to be higher than that of diamond in some cases when basing the thermal conductivity on a difference (ΔT) between the wall temperatures of the evaporator section and the condenser section. The conductivity defined in this way is dependent on length so that for particularly short tube lengths, the advantage of using a heat pipe as a high conductivity thermal bus may not be as great. When coupled with the area enhancement (e.g., via fins) needed to dissipate high heat fluxes at the (relatively small surface area) chip level because of the moderate heat transfer coefficients typical of forced convective air cooling, higher heat dissipation can be derived if a heat pipe is used to form a thermal path between the chip surface and fins. Heat pipes may also be useful as a heat spreader for controlling temperature nonuniformities (Oettinger and Blackburn 1990) on the surface of semiconductor devices (e.g., via "micro" heat pipes (Wu et al. 1990)).

Heat pipes have not found widespread use in commercial applications for cooling either single chips or multi-chip modules due, in part, to economic considerations (e.g., manufacturing costs) and concerns over their long-term reliability. However, improvements in manufacturing capabilities have advanced the state-of-the-art to where heat pipe modules can be cost effective for many applications, and they have high long-term reliability (Waller 1985; Dunn and Reay 1982).

For low evaporator surface temperatures (< 100°C) relevant to chip cooling applications, Babin and Peterson (1990) have tested a heat pipe capable of dissipating high fluxes (> 125 W/cm^2) and maximum total powers of about 65 W. Chao (1990) demonstrated the capability for dissipating up to 250 W using

Contributed by the Electrical and Electronic Packaging Division for publication in the Journal of Electronic Packaging. Manuscript received by the EEPD August 11, 1991; revised manuscript received October 1, 1992. Associate Technical Editor: W. Black.

a finned tube heat pipe design, but a relatively large evaporator area limited heat fluxes to under 10 W/cm^2. Basiulis et al. (1986) tested flat plate heat pipes for cooling printed wiring boards and reported total power dissipations of up to 100 W of power input and fluxes of under 2 W/cm^2.

For "high end" applications that are characterized by the need to simultaneously dissipate high heat flux (>30 W/cm^2) and high total power (on the order of about 1000 W) while maintaining surface temperatures under about 100°C, little work has been reported in the open literature on the use of heat pipes. In the present work, two heat pipe designs are used to demonstrate this capability. Both were designed with a relatively large condenser surface area and a very short adiabatic section common to generic heat pipe designs. The heat dissipating capabilities were thought to be improved as a result by reducing the flow resistance of condensate return to the evaporator section. One of the heat pipes was designed for forced convective air cooling in the condenser section and the other was designed for liquid cooling. The air cooled heat pipe has a "manifold" structure consisting of a base plate in which an array of holes are milled into it which are lined with a wick, and normal to which is attached a tube bundle that forms the condenser section. The base plate serves as a manifold for the condenser tubes. An array of fins is attached to the tube bundle to enhance heat transfer in the condenser. The other heat pipe studied used liquid cooling for the condenser section. It was a "disk" shaped structure in which heat was input over a circular area on one side of the disk. It operated similar to a thermosyphon containing a wick. Liquid (water) cooling in the condenser section was by an array of channels placed around the disk.

2 Experiment

2.1 Manifold Heat Pipe. The manifold design (Fig. 1) consists of an array of holes drilled lengthwise and crosswise into the edge of a copper plate (the manifold evaporator section). The crosswise holes did not penetrate the middle lengthwise hole as shown in Fig. 1. Each of the holes is lined with a wicking material which consisted of sintered copper (Thermacore, Inc., Lancaster, Pa) with a porosity of about 50 percent and a permeability of 2.81 × 10^{-8}cm^2. The effective capillary radius of curvature (length scale of a pore opening) was 23 μm. The wick thickness was 0.79 mm for the holes drilled in the copper plate. The wick thickness in the condenser tubes was 0.64 mm. A wick-lined tube bundle is attached normal to the manifold which forms the condenser section as shown in Fig. 1(*a*). A linear array of five condenser tubes was interconnected with one each of three holes drilled into the base plate in the length-wise direction thus forming three regions in the manifold for evaporation. Figure 1(*b*) illustrates the assumed vapor/liquid flow paths. The total of fifteen condenser tubes (0.81 mm thick wall, 6.4 mm in diameter) were attached to an array of forty one fins of thickness 0.25 mm placed at a pitch of 1.32 mm.

The heat pipe was filled with approximately 8 g of water as the working fluid. This mass of water was sufficient to just saturate the wick. Liquid is evaporated in the base plate and enters the tube bundle where the vapors are condensed by forced air cooling of the fin and tube bundle. The condensate is returned to the base plate by the combined action of gravity and the capillary action of the wick in the condenser tubes.

A wind tunnel test facility was constructed to provide directed air flow through the fin array. A schematic of this setup is shown in Fig. 2. It consisted of a blower, expansion section, settling chamber, nozzle section and a section to provide a transition from a round to a rectangular opening. An array of screens and flow straighteners (honeycomb) were placed in these sections to insure that the flow entering the fin array was nearly uniform. The heat pipe was mounted in the test section of the wind tunnel in the crosswise (shorter) direction so that cooling air encountered each of the three heat pipe sections of the manifold heat pipe in series. To accommodate any mismatch between the fins and the wall and thus prevent any jetting of the cooling air flow along the walls, a rubber sheet was placed between the fins and the walls of the wind tunnel to force the cooling air to go through the fin stack.

The wind tunnel was instrumented with two pitot static tubes and two thermocouples for measuring upstream and downstream velocity, temperature, and static pressure difference. The pitot probes were placed 7.0 cm upstream and 12.5 cm downstream of the entrance and exit to the fin array. The probes were mounted in such a way that they could be easily traversed over the cross section of the wind tunnel. The probes were positioned over a grid consisting of twenty three locations across the width of the wind tunnel (14.0 cm) and five locations over the height (5.7 cm). Each location was considered the center of a "cell" in which the velocity and mass flow rate were determined based on the pressure and temperature measurement within the cell. The total mass flow rate of air was determined by summing the mass flow rates through each of the cells. In the present study, air flow rates of .0094 kg/s and .05 kg/s (the highest achievable with the blower used corresponding to a maximum entrance air velocity to the fin array of 5.3 m/s) are reported. The corresponding air velocities, based on the total cross sectional area of the wind tunnel, were .7 m/s and 5.3 m/s, respectively. Additional results are provided elsewhere (North 1993).

A copper block containing three cartridge heaters was used to provide heat to the manifold plate over a square area 4.45 cm on a side. A layer of thermal grease (GC Electronics, Rockland, Ill.) was placed between the heater block and the heat pipe surface to minimize the contact resistance between the two surfaces. The heat flux into the heat pipe manifold plate was determined by measuring the temperature gradient within the copper block. The temperature gradient was deter-

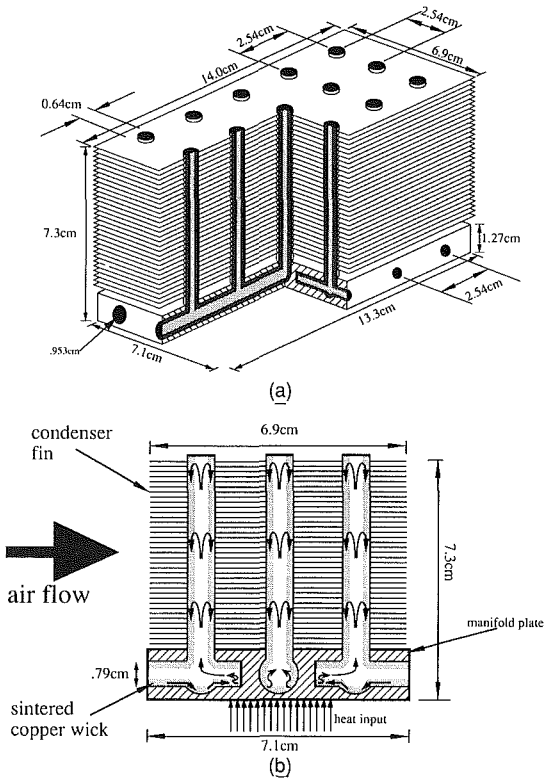

Fig. 1 The manifold heat pipe (*a*) perspective view; (*b*) cross section illustrating vapor and liquid flow paths

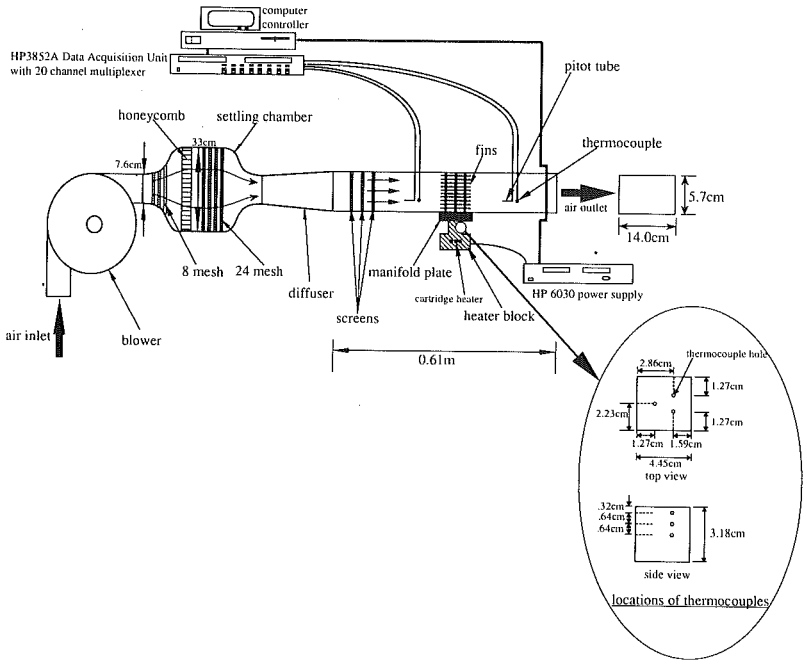

Fig. 2 Schematic diagram of the wind tunnel test facility for the manifold heat pipe

mined at three locations in the block and was constructed from three temperature measurements at different depths within the block. The inset to Fig. 2 shows the locations of the thermocouples. Surface heat fluxes calculated from temperature distributions extrapolated to the surface were within 3 percent of each other. Thus, the heat flux into the manifold heat pipe was essentially uniform.

Surface temperatures on the heat pipe were measured with 0.25 mm diameter thermocouples placed in grooves cut into the heat pipe surface under the heater. One thermocouple was placed at the center of the heater and four more were placed at the corners of a square 3.18 cm on a side, also concentric with the heater. These locations are identified in the inset of Fig. 6. Extrapolated surface temperatures in the heater block typically differed from each other, and from the measured surface temperatures of the heat pipe surface, by less than a degree thus indicating good thermal contact between the heater and heat pipe surface. The heat fluxes were determined from the average of the three measured gradients. The heat fluxes inferred from the temperature gradient differed from the heat input based on the electrical power input to the heat pipe by under 10 percent, with the difference being a measure of heat losses through the insulation.

A computer-based data acquisition system (HP 3852A 20 channel multiplexer connected to a PC) was used to control power input to the heater and to monitor the output from all thermocouples. Power input was provided in fixed steps of 30 W each. All temperatures were sampled at a rate of at least once every 40 s. After steady state was achieved, the power to the heaters was incremented by the programmed value until a new steady state temperature was achieved. Power was incremented in this way well into what was believed to be the dryout regime in order to clearly identify if dryout had occurred or until limitations on either the heater or power supply were reached. A typical experimental run lasted between twelve and twenty four hours.

Experimental errors and uncertainties arose principally with two measurements: temperatures and air flow rates in the wind tunnel. The uncertainty of all temperature measurements (including those made for the disk heat pipe-Section 2.2) was estimated to be 1.3°C based on uncertainty in the calibration of the thermocouple material. All thermocouples used in this study were type *K* and manufactured by Omega, Inc. (Stamford, CT.). The uncertainty in the measured air velocity within the wind tunnel was estimated to be a maximum of 10 percent at the highest velocity studied-5.3 m/s (.05 kg/s) ± .5 m/s. This uncertainty was attributed to pressure fluctuations recorded by the pitot probes. The air flow was turbulent as the corresponding Reynolds number ranged from about 4000 to 30,000. At the lowest air velocity studied of .7 m/s (.0094 kg/s) the pressure fluctuations were noticeably reduced.

2.2 Disk Heat Pipe. The disk heat pipe (Fig. 3) consisted of two copper plates sandwiched around a cylinder with a length of 2.54 cm and an ID 14.9 cm. The two plates were coated with sintered copper powder (manufactured by Thermacore, Inc.) which served as the wick material. The sintered coating was 3 mm thick. The effective capillary radius of curvature was 36 μm, and the porosity and permeability were approximately 50 percent, and 2.1 $\times$ 10^{-7}cm^2, respectively. These values were chosen to optimize the liquid return to the region of heat addition to the heat pipe (Pruzan et al. 1991).

Heat was input over a 7.62 cm diameter area at the center of the bottom plate. The remainder of the heat pipe was surrounded by a cooling water jacket. Results are reported here for one water flow rate: .032 kg/s at an inlet water temperature of 25°C. The working fluid was ethanol. Condensation of ethanol occurred on the top plate, the side walls, and the outer edge of the lower plate. No wick material was placed on the side walls of this heat pipe so that it was designed primarily for operation normal to gravity. Experiments are reported with the disk heat pipe filled with either 39 g (50 cm^3) or 92 g (116 cm^3) of ethanol, representing approximately 13 and 29 percent, respectively, of the total void volume (accounting for the porosity of the sintered wick and the volume of the vapor space). These quantities of working fluid were chosen so that the wicks would be just saturated with liquid and completely flooded with liquid to twice the thickness of the wick, respectively, in the power-off state.

Temperatures in the evaporator section were monitored by four 0.25 mm sheathed thermocouples which were placed in grooves cut into the copper surface of the heat pipe. The fit between the thermocouples and grooves was tight for good

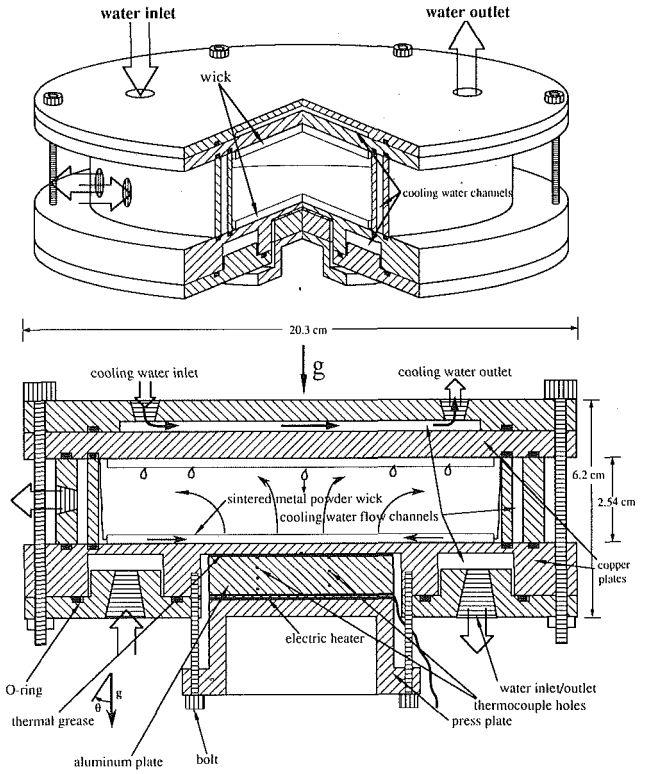

Fig. 3 The disk heat pipe (*a*) perspective view; (*b*) cross sectional view illustrating anticipated liquid and vapor flow paths

thermal contact. Results are reported here for a thermocouple located at the center of the evaporator circle. Surface temperatures at other locations are included elsewhere (North 1993).

A 1.27 cm thick aluminum disk was placed between the heater and heat pipe and instrumented with thermocouples in order to directly measure the temperature gradient at two locations 0.635 cm from the disk center and to thus get an indication of the spatial variation of heat flux. The bottom thermocouple in the disk was fit into a groove similar to the grooves cut into the copper surface so that the two thermocouple junctions were less than 0.2 cm apart. The resulting thermal contact resistances were inferred to be approximately .2 cm^2 – °C/W and 1.4 cm^2 – °C/W for the two locations monitored. Also, the heat flux into the aluminum disk was not uniform because only approximately 76 percent of the surface area of the heater (Minco Products, Minneapolis, Mn., No. HM6808 electric heater) actively dissipated heat. A meaningful average heat flux could thus not be determined from the measured temperature gradient. However, the difference between the total electrical power input to the heater and the enthalpy increase of the cooling water was less than 5 percent for all runs. Thus, the area averaged fluxes obtained from the electrical power input were used in the presentation of the results.

The same computer data acquisition system as for the manifold heat pipe was used to control power input to the heater and to monitor the output from all thermocouples and the flow transducer for the disk heat pipe. Power input was provided in fixed steps of 50 W at regular intervals. Several trial runs established that steady state temperatures could be achieved within one hour for all power levels below the dryout heat flux for the manifold heat pipe and within 30 min for the disk heat pipe.

3 Results

The performance of the heat pipes are represented by displaying the variation of input heat flux with surface temperature-a "performance" curve. The performance curves were constructed from data of the type shown in Figs. 4 and 5. These figures display the evolution of surface temperature for a series of incremented heat fluxes for a typical run of the manifold (Fig. 4 for an air flow rate of .05 kg/s) and disk (Fig. 5 for a cooling water flow rate of .032 kg/s) heat pipes.

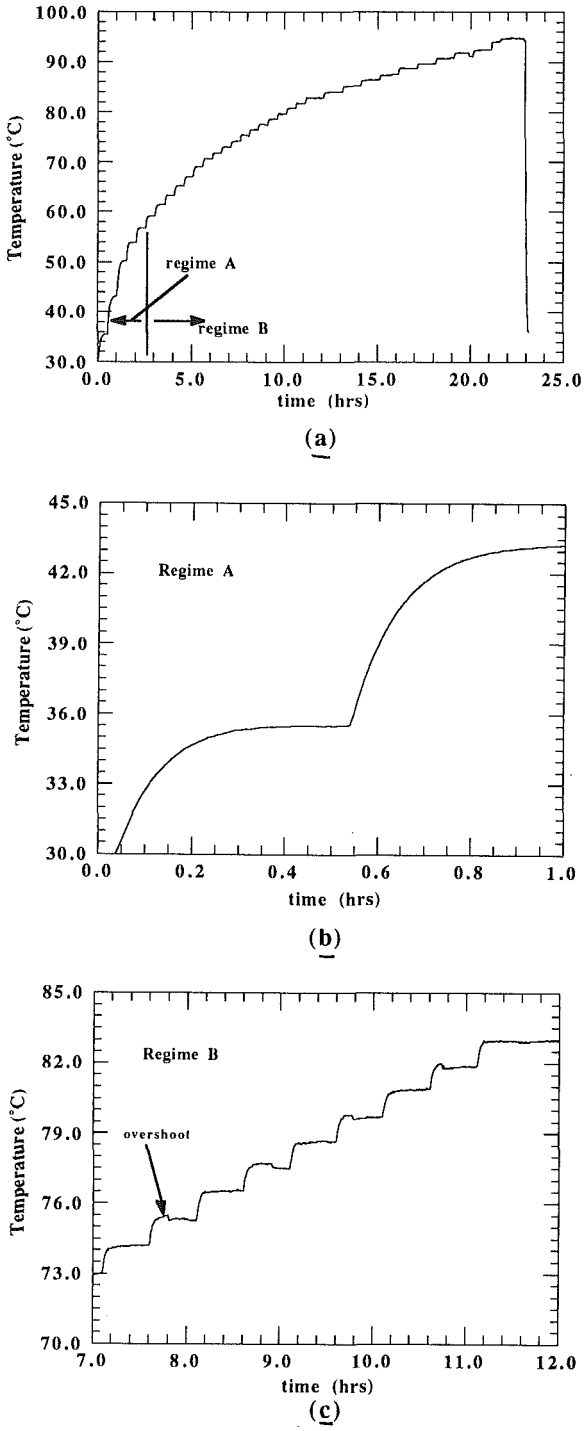

Fig. 4 Evolution of surface temperature of the manifold heat pipe. Ambient air temperature, and inlet air temperature to the condenser fin array, was 27C and 0.05 kg/s (corresponding to an air velocity of 5.3 m/s), respectively. Stepwise temperature increases reflect a transient temperature followed by a steady state temperature after a power increment of 30 W. (*a*) regimes *A* and *B* are indicated for a complete experimental run; (*b*) regime *A* illustrating smooth evolution of temperature; (*c*) regime *B* illustrating overshoot of temperature that may be indicative of boiling in the wick.

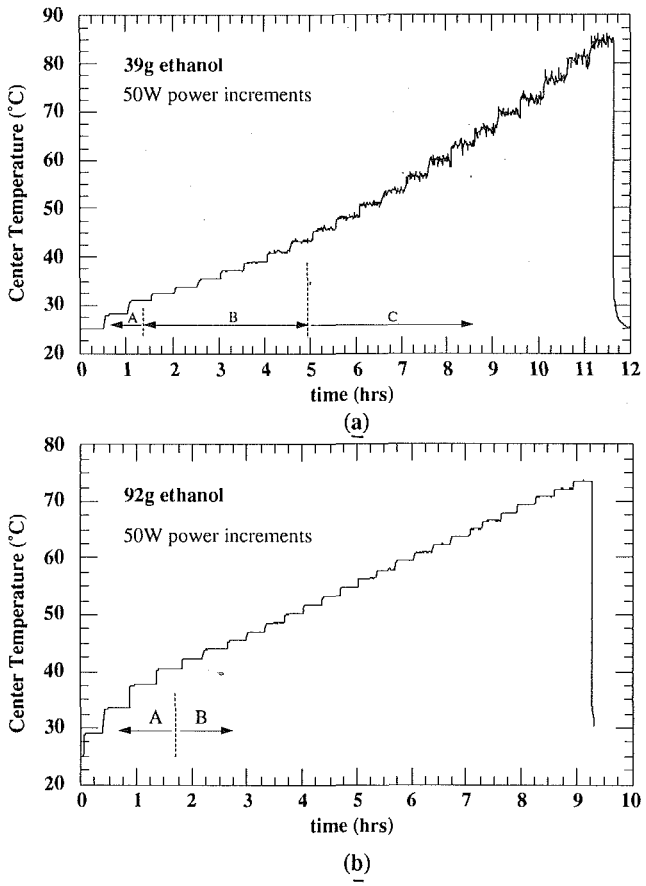

Fig. 5 Evolution of surface temperature of the disk heat pipe. Inlet water temperature was 25C. Stepwise temperature increases reflect a transient temperature followed by a steady state temperature after a power increment of 50 W. (*a*) 39 g ethanol in the heat pipe illustrating temperature oscillations that may be indicative of dryout; (*b*) 92 g ethanol in the heat pipe. Approximate locations of regimes *A*, *B*, and *C* are indicated.

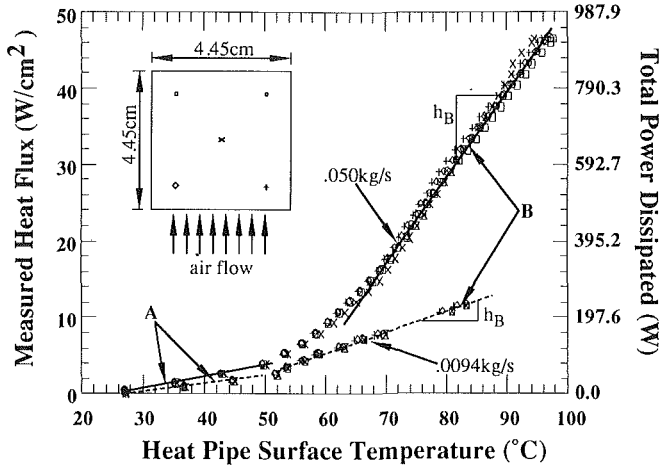

Fig. 6 Variation of input heat flux with surface temperature for the manifold heat pipe at two different air flow rates. Surface temperature locations are indicated in the inset and identified by the respective symbols. Regimes *A* and *B* are indicated as well as the total power input to the heat pipe on the right-hand axis.

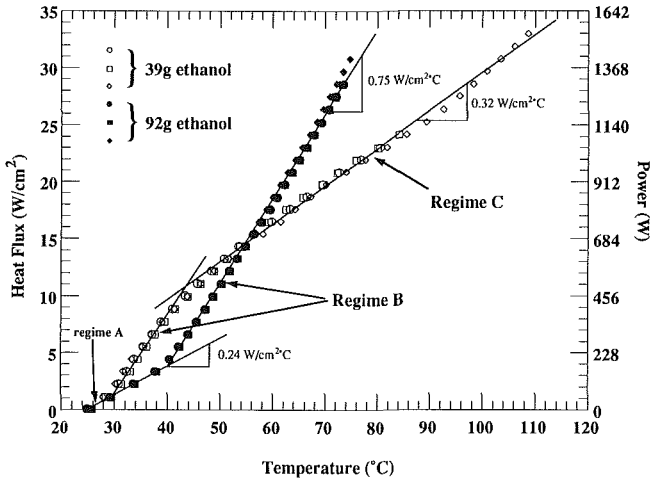

Fig. 7 Variation of input heat flux with surface temperature at the center of the area of heat input for the disk heat pipe at fluid charges of 39 g and 92 g. Data for three different experimental runs are indicated to illustrate repeatability. Initiation of regime *C* for dryout corresponds to the onset of temperature oscillations (cf, Fig. 5(*a*) for the 39 g fluid charge). The total power input to the heat pipe is given on the right-hand axis.

The steps shown are the result of incrementing the power input. Steady state is indicated by the horizontal portions of the curve for each power step. The decrease in temperature at the right hand side of Figs. 4(*a*) and 5 is the result of power to the heater being shut off at the conclusion of the experimental run.

Two regimes are believed to be revealed in Fig. 4 for the manifold heat pipe corresponding to the maximum air flow rate studied of .05 kg/s: 1) a single phase regime ("*A*"), and 2) a boiling regime ("*B*"). Results similiar to those shown in Fig. 4 were observed at lower air flow rates but are not reported here (North 1993). The single phase regime was characterized by temperature achieving a steady state value without overshoot (cf, Fig. 4(*b*)). In this regime the temperature increase corresponding to each step in input power (30 W) was about 7°C. The primary mode of heat dissipation in this regime is probably evaporation at the liquid/vapor interface, and only liquid exists within the wick. Boiling is thought to occur in the wick in regime B (cf. Fig. 4(*c*)). In regime B the temperature increase for each step (about 1°C) was smaller than measured for regime *A* which is consistent with more effective heat transfer inherent in the boiling process; a small temperature overshoot was observed at some power levels.

Figure 5 shows representative temperature-time histories of the disk heat pipe at the center location of the evaporator for power steps of 50 W. Results for a fluid charge of 39 g are shown in Figs. 5(*a*), and Fig. 5(*b*) shows results for 92 g of ethanol in the heat pipe. With both charges of working fluid in the disk heat pipe, trends similar to those seen in the manifold heat pipe were observed.

Oscillations of temperature for the 39 g charge of ethanol (Fig. 5(*a*)) may have been due to intermittent wetting of the wick which signal the onset of dryout in the disk heat pipe. By contrast, with 92 g of ethanol in the heat pipe (Fig. 5(*b*)), there was no evidence of temperature oscillations over the entire range of power settings examined. With the higher fluid charge, the wick was most likely submerged in ethanol at all power levels studied.

Figure 6 illustrates the performance curve for the manifold heat pipe for all five of the locations monitored in the evaporator section for air flow rates of .0094 kg/s and .05 kg/s. The total power input to the heater is also shown in Fig. 6. The lines in this (and Fig. 7) were drawn to suggest trends. The results show that the heated section is nearly isothermal. The heat dissipation rate is strongly dependent on the air flow rate through the fin array as expected, with the higher air flow rate yielding lower temperatures and higher heat fluxes than the lower flow rate.

The regimes that are believed to be indicative of *A* and *B* are shown in Fig. 6 (cf, Fig. 3). The boundary between these regimes is identified by a change in the derivative $\partial q_j'' / \partial T$ which is also a measure of the heat transfer coefficient h_j in regime "*j*" (*A* or *B*) and where q_j'' is the corresponding heat flux and

T is the surface temperature. For example, for an air flow rate of .05 kg/s, $h_A \approx 0.16$ W/(cm^2 – °C) and $h_B \approx 1.09$ W/(cm^2 – °C). Heat transfer in regime B is thus about six times more effective in dissipating heat than regime A for the same surface temperature. No evidence of dryout was found for the range of input powers and air flow rates studied for this heat pipe. The upper limits shown in Fig. 6 were determined by limitations on the power supply used.

Figure 7 shows the performance curves of the disk heat pipe for fluid charges of 39 g and 92 g and for a water flow rate of .032 kg/s. The total power is also indicated. Data for three separate runs are shown for each of the fluid charges. The small scatter in the data demonstrates the repeatability of the operation of this heat pipe. While only the center temperature is indicated in Fig. 7, surface temperatures at other locations in the heated section were within a few degrees of the temperature displayed in Fig. 7 which suggests that the heated section was nearly isothermal.

The variation of heat flux with surface temperature is nearly linear for the regimes suggested by the curves, similar to the operation of the manifold heat pipe. For a fluid charge of 92 g, regimes A and B can be discerned, with $h_A \approx 0.24$ W/(cm^2 – °C) and $h_B \approx 0.75$ W/(cm^2 – °C). High heat fluxes (> 30 W/cm^2) and high total powers (> 1400 W) are shown at low surface temperatures (< 80°C) for the 92 g fluid charge. No evidence of dryout was revealed at the highest power input (the limits of the power supplies used) with the 92 g charge, while it is believed that the results shown in Fig. 7 suggest that dryout may have occurred with the 39 g fluid charge.

For 39 g of ethanol in the heat pipe, regimes A and B are not as clearly defined as for the 92 g charge. The extent of regime A was relatively small. Regime B extended between about 2 W/cm^2 to 8 W/cm^2 with $h_B \approx 0.74$ W/(cm^2 – °C). Above about 10 W/cm^2, a third regime ("C") could be identified which is believed to be due to dryout of the wick. In regime C, $h_C \approx .32$ W/(cm^2°C) which reflects the diminished ability of the wick to remove heat without being saturated with the coolant. A discontinuous drop in the heat transfer coefficient, also termed a "knee" in the performance curve (Babin and Peterson 1990), is consistent with its interpretation in terms of dryout (Pruzan et al. 1990). The beginning of regime C in Fig. 7, at a surface temperature of about 45°C, appears to coincide with temperature oscillations in the wick (cf, Fig. 5(a)) as discussed above.

Even though dryout may be suggested by the trends discussed above for 39 g of ethanol in the disk heat pipe, the surface temperatures are still low. This fact is probably due to efficient cooling provided by the water channels which are immediately adjacent to the heated section (cf, Fig. 3). If dryout is in fact suggested by the results in Fig. 7 for the 39 g fluid charge, heat conduction in the heat pipe housing toward the lower cooling channel is still apparently good enough for the design shown in Fig. 3 to maintain surface temperatures below 100°C up to input heat fluxes of over 25 W/cm^2.

4 Conclusions

Two heat pipe designs have been tested which have the capability of dissipating high heat fluxes (> 30 W/cm^2) and high total power while maintaining low surface temperatures (< 100°C). One of the heat pipes utilized an air cooled condenser section, while the other employed liquid cooling (water). Lower surface temperatures were observed with the liquid cooled heat pipe. Both designs were characterized by a virtual absence of an adiabatic section traditional to heat pipe designs.

The highest steady state heat flux measured for the disk heat pipe was about 31 W/cm^2 and the total power input was over 1400 W when the surface temperature was 75°C and the inlet cooling water temperature was 25°C. It is plausible that higher fluxes could be reached by lowering the temperature of the cooling water.

A steady state flux of over 47 W/cm^2 was achieved with the manifold heat pipe with 0.050 kg/s of ambient cooling airflow channeled through the fin array. The maximum surface temperature observed was 93°C with 27°C cooling air and the total power dissipated was over 900 W. The physical size of this heat pipe is small enough that it could fit inside a desktop package.

Acknowledgments

Conversations with Mr. Ehsan Ettehadieh of Sun Microsystems, Messrs. Robert M. Shaubach and Brian Fritsch of Thermacore, Inc., Profs. Kenneth E. Torrance and Che-Yu Li of Cornell University, Prof. Roop L. Mahajan of the University of Colorado, Boulder, and Mr. Algerd Basiulis of Hughes Aircraft Co. were beneficial to the completion of this study. The manifold heat pipe was designed by Sun Microsystems and constructed by Thermacore, Inc.

Financial support for this work was provided by the Semiconductor Research Corporation, the National Science Foundation (grant No. CBT-8451075), and the Industry-Cornell University Alliance for Electronic Packaging.

References

Andros, F. E., and Sammakia, B., 1989, "Thermal Management of Electronic Packaging," *Principles of Electronic Packaging* (D. P. Seraphim, R. Lasky, and C. Y. Li, eds.) McGraw-Hill, New York, pp. 127–158.

Antonetti, V. W., Oktay, S., and Simons, R. E., 1989, "Heat Transfer in Electronic Packaging," in *Microelectronics Packaging Handbook* (R. R. Tummala and E. J. Rymaszewshi, eds.), van Nostrand & Reinhold, New York, pp. 167–223.

Babin, B. R., and Peterson, G. P., 1990, "Experimental Investigation of a Flexible Bellows Heat Pipe for Cooling Discrete Heat Sources," *J. Heat Trans.*, Vol. 112, pp. 602–607.

Basiulis, A., Tanzer, H., and McCabe, S., 1986, "Thermal Management of High Power PWBs Through the Use of Heat Pipe Substrates," *Proc. 6th Ann. Intl. Elect. Pack. Conf.*, pp. 501–515.

Bergles, A. E., 1988, "High Flux Boiling Applied to Microelectronics Thermal Control," *Int. Comm. Heat Mass Trans.*, Vol. 15, pp. 509–531.

Chao, S., 1990, "Thermal Management of High-Power Tab IC Chips Incorporating Heat Spreaders and Heat Pipes," *Proc. 9th Intl. Heat Trans. Conf.*, Vol. 2, pp. 295–300.

Dunn, P. D., and Reay, D. A., 1982, *Heat Pipes*, 3rd edition, Pergamon Press, New York, pp. 103–113.

Faghri, A., and Buchko, M., 1991, "Experimental and Numerical Analysis of Low-Temperature Heat Pipes with Multiple Heat Sources," ASME *Journal of Heat Transfer*, Vol. 116, pp. 728–734.

Hanneman, R., 1989, "Thermal Control for Mini and Microcomputers: The Limits of Air Cooling," *Bull. Int. Cent. Heat Mass Trans.*, Vol. 3, pp. 65–83.

Kraus, A. D., and Bar-Cohen, A., 1983, *Thermal Analysis and Control of Electronic Equipment*, McGraw-Hill, New York.

North, M. T., 1993, Ph.D. thesis, Cornell University, Ithaca, New York.

Oettinger, F. F., and Blackburn, D. L., 1990, "Thermal Resistance Measurements," *NIST Special Publication* 400-86, U.S. Government Printing Office, Washington, D.C., July.

Ponnappan, R., Ramalingam, M. L., Johnson, J. E., and Mahefkey, E. T., 1989, "Evaporator Critical Heat Flux in the Double-Wall Artery Heat Pipe," *Experimental Thermal and Fluid Science*, Vol. 2, pp. 450–464.

Pruzan, D. A., Klingensmith, K. A., Torrance, K. E., and Avedisian, C. T., 1991, "Design of High-Performance Sintered-Wick Heat Pipes," *Int. J. Heat Mass Trans.*, Vol. 34, pp. 1417–1427.

Pruzan, D. A., Torrance, K. E., and Avedisian, C. T., 1990, "Two-Phase Flow and Dryout in a Screen Wick Saturated with a Fluid Mixture," *Int. J. Heat Mass Trans.*, Vol. 33, pp. 673–681.

Waller, L., 1985, "An Old Idea May Solve VHSIC Cooling Problem," *Electronics*, pp. 19–20, Aug.

Wu, D., Peterson, G. P., and Chang, W., 1990, "Experimental Investigation of the Transient Behavior of Micro Heat Pipes," *AIAA Paper No. 90-1791.*